ELSEVIER

Synthetic sandwich culture of 3D hepatocyte monolayer

Yanan Du[a,b,1], Rongbin Han[a,b,1], Feng Wen[a,b], Susanne Ng San San[a,b], Lei Xia[a,b],
Thorsten Wohland[b,d], Hwa Liang Leo[a,*], Hanry Yu[a,b,c,e,f,g,**]

[a]*Institute of Bioengineering and Nanotechnology, A*STAR, Singapore 138669, Singapore*
[b]*Graduate Programme in Bioengineering, Graduate School for Integrative Sciences and Engineering, National University of Singapore, Singapore 117597, Singapore*
[c]*Department of Physiology, Yong Loo Lin School of Medicine, National University of Singapore, Singapore 117597, Singapore*
[d]*Department of Chemistry, Faculty of Science, National University of Singapore, Singapore 117543, Singapore*
[e]*Singapore-MIT Alliance, E4-04-10, 4 Engineering Drive 3, Singapore 117576, Singapore*
[f]*NUS Tissue-Engineering Programme, DSO Labs, National University of Singapore, Singapore 117597, Singapore*
[g]*Department of Haematology–Oncology, National University Hospital, Singapore 119074, Singapore*

Abstract

The sandwich culture of hepatocytes, between double layers of extra-cellular matrix (ECM), is a well-established *in vitro* model for re-establishing hepatic polarity and maintaining differentiated functions. Applications of the ECM-based sandwich culture are limited by the mass transfer barriers induced by the top gelled ECM layer, complex molecular composition of ECM with batch-to-batch variation and uncontrollable coating of the ECM double layers. We have addressed these limitations of the ECM-based sandwich culture by developing an 'ECM-free' synthetic sandwich culture, which is constructed by sandwiching a 3D hepatocyte monolayer between a glycine-arginine-glycine-aspatic acid-serine (GRGDS)-modified polyethylene terephthalate (PET) track-etched membrane (top support) and a galactosylated PET film (bottom substratum). The bioactive top support and bottom substratum in the synthetic sandwich culture substituted for the functionalities of the ECM in the ECM-based sandwich culture with further improvement in mass transfer and optimal material properties. The 3D hepatocyte monolayer in the synthetic sandwich culture exhibited a similar process of hepatic polarity formation, better cell–cell interaction and improved differentiated functions over 14-day culture compared to the hepatocytes in collagen sandwich culture. The novel 3D hepatocyte monolayer sandwich culture using bioactive synthetic materials may readily replace the ECM-based sandwich culture for liver tissue engineering applications, such as drug metabolism/toxicity testing and hepatocyte-based bioreactors.
© 2007 Elsevier Ltd. All rights reserved.

Keywords: Sandwich culture; Hepatocyte; Synthetic materials; Polarity; RGD peptide; Galactosylation

1. Introduction

In vivo, hepatocytes are organized into a polarized epithelium with distinct apical (bile canalicular) and basal (sinusoidal) domains [1]. The basal domain of the hepatocytes is in contact with a complex extracellular matrix (ECM) containing fibronectin, laminin, collagen I–V, and proteoglycans in the space of Disse [2]. The interactions of hepatocytes with the ECM environment are important for hepatic polarity and differentiated function maintenance [3]. In standard *in vitro* culture, primary hepatocytes cultured on substrates coated with ECM protein, such as collagen or fibronectin, typically exhibit spreading morphology with deteriorating differentiated functions and nearly no polarized structure [4]. This deteriorating process could be rescued by overlaying another ECM layer, such as collagen or basement membrane (Matrigel[TM]), which mimics the ECM distribution in the space of Disse. Hepatocyte

*Corresponding author. Tel.: +65 65163466; +65 68247103; fax: +65 68727150.
**Also for correspondence
E-mail addresses: hlleo@ibn.a-star.edu.sg (H.L. Leo), phsyuh@nus.edu.sg (H. Yu).
[1]These authors contribute equally to this work.

sandwich culture between double layers of ECM is an *in vitro* model with re-established hepatic polarity and stable differentiated functions [3,5,6]. The hepatocyte sandwich culture has been adopted in liver physiology studies [7,8], drug metabolism/toxicity testing [9] and hepatocyte-based bioreactors [10,11]. Further applications of the conventional ECM-based sandwich culture were hampered by the complex molecular compositions of the ECM with batch to batch variation [12], uncontrollable ECM coating, mass transfer barriers induced by the gelled ECM-coated top support (hindering the exchange of nutrients, xenobiotics or biochemical signals with the bulk culture medium), and shedding of the ECM coating from the top support during culture. In this study, we have addressed these limitations of the ECM-based sandwich culture by developing an 'ECM-free' synthetic sandwich culture, in which we replaced the natural ECM with bioactive polymeric materials to achieve improved mass transfer and stable differentiated functions.

A variety of synthetic substrata with bioactive components, such as cell adhesion peptides: Arg-Gly-Asp (RGD) [13], Tyr-Ile-Gly-Ser-Arg (YIGSR) [14], Gly-Phe-Hyp-Gly-Glu-Arg (GFOGER) [15] or sugar ligands: galactose [16], glucose [17], lactose [18], have been used for cell culture to replace natural ECM with well-controlled material properties and cellular responses. Previously, we have fabricated a galactosylated polyethylene terephthalate (PET-Gal) film for primary rat hepatocyte culture and identified a 3D hepatocyte monolayer formed on the PET-Gal [19]. The 3D hepatocyte monolayer exhibited 3D cellular structure and polarities, enhanced cell–cell interactions and differentiated functions compared to the 2D hepatocyte monolayer on collagen-coated substratum [19]. Here, we established a synthetic sandwich culture by overlaying the 3D hepatocyte monolayer on the PET-Gal (bottom substratum) with a porous PET track-etched (TE) membrane (top support). Since the biochemical compositions of ECM play essential roles in regulating hepatocyte morphology, polarity and differentiated functions in ECM-based sandwich culture [20–22], we investigated the influence of three different top support (galactosylated, GRGDS-modified or non-modified PET TE membrane) on the hepatocyte morphology, polarity and differentiated functions in the 3D hepatocyte monolayer of the synthetic sandwich culture. The synthetic sandwich culture with GRGDS-modified PET TE membrane (top support)/PET-Gal (bottom substratum) exhibited the optimal performances, in terms of stabilizing the 3D monolayer morphology, re-establishing hepatocyte polarity and maintaining other differentiated functions.

We compared this GRGDS-modified PET TE membrane/PET-Gal synthetic sandwich culture of 3D hepatocyte monolayer with the collagen sandwich hepatocyte culture. 3D hepatocyte monolayer in the synthetic sandwich culture exhibited similar dynamic process of polarity formation and biliary excretion, improved mass transfer, enhanced cell–cell interaction, differentiated functions compared with the hepatocytes in the collagen sandwich culture. This synthetic sandwich culture model can replace the ECM-based sandwich culture for relevant hepatocyte-based applications such as drug metabolism/toxicity testing and hepatocyte-based bioreactors [7,8].

2. Materials and methods

2.1. Materials

PET TE membranes with thickness of 9 μm, pore density of 3×10^7 pores/cm^2 and pore diameter of 0.8 μm were purchased from Sterlitech (WA, USA). The galactose ligand, 1-*O*-(6′-aminohexyl)-D-galactopyranoside (AHG, M.W. 279) was synthesized previously [23–25]. GRGDS peptide was purchased from Peptides International (Kentucky, USA). Minusheet carriers were purchased from Minucells and Minutissue Vertriebs GmbH (Bad Abbach, Germany). Primary rabbit anti-E-Cadherin and anti-GAPDH antibody were purchased from Santa Cruz (CA, USA). All other chemicals were purchased from Sigma-Aldrich Singapore unless otherwise stated.

2.2. Fabricating PET-Gal as the bottom substratum

PET-Gal was fabricated as reported previously [26,27], which was cut into circular disks with diameter of 12 mm in order to fit into minusheet carriers.

2.3. Fabricating galactosylated or GRGDS-modified PET TE membrane as the top support

Circular disk of the non-modified PET TE membrane with diameter of 12 mm was functionalized by generating carboxylic groups directly from the TE polyester bulk material using a revised protocol [28]. Briefly, the non-modified PET TE membrane was oxidized with KMnO$_4$ in 1.2 N H$_2$SO$_4$ (50 g/L) at 60 °C for 1 h followed by rinsing successively with 6 N HCl (2 × 30 min) and DI water (3 × 10 min). For GRGDS peptide or galactose ligand (AHG) conjugation, 300 μL of MES buffer (50 mM, pH of 5.5) containing 10 mg EDC and 2 mg sulfo-NHS was added to each well of the 24-well plate containing the PET TE membrane to activate the carboxylic groups by forming NHS esters. After 2 h activation at room temperature (RT), the MES solution was completely removed and replenished with 300 μL phosphate buffer (0.1 M, pH of 7.4) containing ligands (0.2 mg GRGDS peptide or 1 mg AHG) and allowed to react for 48 h at 4 °C under shaking. After reaction, each membrane was blocked with 0.5% ethanolamine solution for 15 min to quench non-specific interactions due to the un-reacted carboxylic groups. All substrata were sterilized by soaking with 70% ethanol for 3 h and then rinsed 3 × with PBS before cell culture.

2.4. Characterization of the bioactive PET film and PET TE membrane

The density of carboxylic groups on the PET film or PET TE membrane was determined by a colorimetric method using Toluidine Blue O (TBO) [25,29].

X-ray photoelectron spectrometry (XPS) was used to qualitatively determine the surface chemical composition as described previously [26]. All binding energies were referenced to the C 1s hydrocarbon peak at 284.6 eV and peak deconvolution was performed by software XPSPEAK Version 4.1 with linear background correction [25].

The density of the GRGDS or galactose ligands on PET TE membrane was quantified by reverse phase-HPLC (RP-HPLC) developed previously [26]. Briefly, the conjugated ligands were hydrolyzed off the membrane using an Acid Hydrolysis Station (C.A.T. GmbH & Co.). The cooled

hydrolyzed solution was filtered into a new vial and evaporated under nitrogen. The hydrolyzed ligands from the membrane were re-suspended in DI-water and derivatized using ATTO-TAG[TM] CBQCA Amine-Derivatization Kit (Molecular Probes) for fluorescence detection by RP-HPLC (Agilent Technology).

2.5. Hepatocyte isolation and culture

Hepatocytes were harvested from male Wistar rats by a two-step in situ collagenase perfusion method [30]. Viability of the hepatocytes was determined to be >90% with a yield of >10^8 cells/rat.

Freshly isolated hepatocytes were seeded onto different substrata in 24-well plate at the density of 10^5 cells/cm^2 and cultured in William's E culture medium supplemented with 1 mg/ml BSA, 10 ng/ml of EGF, 0.5 µg/ml of insulin, 5 nM dexamethasone, 50 ng/ml linoleic acid, 100 units/ml penicillin, and 100 µg/ml streptomycin.

In synthetic sandwich culture, hepatocytes were seeded on the PET-Gal for 3 h to achieve full attachment. Culture medium containing the unattached cells was removed; and the attached hepatocytes were cultured in fresh medium for 1 day until the PET TE membrane top support (galactosylated; GRGDS-modified or unmodified) was overlaid. The sandwich construct was secured using the O-rings on the minusheet carriers. In collagen sandwich culture, the bottom collagen-coating substratum was prepared by spotting 40 µl neutralized collagen I solution (Vitrogen, Palo Alto, CA) onto the 12 mm glass coverslip before incubation at 37 °C overnight for gelation. Hepatocytes seeded on the collagen-coated coverslip were incubated for 1 h for full attachment before media replenishment and then cultured for 24 h. The culture medium was removed and a layer of un-gelled collagen was overlaid on top of the cells. Gelation of the collagen overlay was allowed to occur at 37 °C for 3 h before fresh medium was replenished.

2.6. FITC-dextran diffusivity measurement

Measurement of the diffusivity of Fluorescein Isothiocyanate-conjugated dextrans (FITC-dextrans, with molecular weight: 9.5, 70 and 150 kDa) through the various PET TE membrane top supports and collagen top support were based on a donor–receptor compartment model [31]. Briefly, the membrane was clamped between the receptor and donor compartments using minusheet carriers. Donor compartments were filled with 20 µl of 0.2 wt% FITC-dextran in PBS, while receptor compartments were filled with 200 µl of PBS. Samples were taken from the receptor compartment every hour and replaced with fresh PBS. For the measurement of diffusivity of FITC-dextrans through the collagen layer, 20 µl of 0.2 wt% FITC-dextran in PBS was maintained in the glass coverslip and 40 µl of collagen was added at the top. The whole construct was maintained in minucell carriers and incubated for 3 h in 37 °C to facilitate the gelation of collagen. Two hundred microliters PBS was added on the receptor compartment; and samples were taken from the receptor compartment every hour and replaced with fresh PBS. The concentrations of FITC-dextran were measured at 490 nm excitation/525 nm emission against FITC-dextran standards using the microplate reader (Tecan Safire^2, Switzerland).

2.7. Scanning electron microscopy

SEM images were acquired as described previously [19].

2.8. Western blot

Hepatocytes (total cell number >2 millon) in different culture models were lysed; the protein concentration per sample was quantified by Dc protein Reagent assay (Bio-rad, US); 15 µg protein sample per lane was loaded and fractionated by 7.5% SDS–PAGE gel and transferred to a PVDF membrane (Millipore, US) by semi-dry electro-blotting. [19]. The membranes were blocked with 3% non-fat milk in TBS-T for 1 h at RT

and incubated with primary rabbit anti-E-Cadherin (1:500) or rabbit anti-GAPDH (1:1000) overnight at 4 °C. After 5× washing with TBS-T buffer, the membrane was incubated with secondary goat peroxidase-conjugated anti-rabbit or anti-mouse IgG 1:10,000 diluted in 0.5% non-fat milk for 1 h at RT. After 5× washing, the membrane was treated with ELC plus reagent (GE Healthcare, UK); and light emission was detected by Hyperfilm (GE Healthcare, UK). Films were developed in a KODAK Medical X-ray Processor (KODAK, USA) and imaged by a KODAK IMAGE Station 2000MM (KODAK, USA). Relative quantification of western blot was performed by measuring the mean pixel intensity associated with individual bands with PhotoShop 7.0 software. A background noise value was subtracted from each protein band to obtain a corrected mean pixel intensity value.

2.9. Biliary excretion of fluorescein

3 µg/ml of fluorescein diacetate (Molecular Probes, Oregon) was incubated with the hepatocytes at 37 °C for 45 min in culture medium to visualize the biliary excretion of fluorescein [7]. The cells were rinsed and fixed before being imaged under a confocal microscope using a 40× water lens. Image-pro Plus software (MediaCybernetics, USA) was used to process the images and quantify the fluorescein localization in the intercellular sacs between hepatocytes (see supplementary material).

2.10. Immunofluorescence microscopy

For F-actin staining, the cells were fixed using 3.7% PFA, blocked in 10% fetal calf serum (FCS) at RT for 1 h, permeabilized for 5 min in 0.1% Trion X-100 in 1% bovine serum albumin solution (BSA), incubated with TRITC-phalloidin (1 µg/ml) for 20 min and then wash 3× with PBS before imaging. For double-staining of MRP2/CD147, cells fixed with PFA were blocked in 10% FCS for 1 h at RT. Samples were incubated with the primary anti-CD147 monoclonal antibody (Serotec, Raleigh) and primary anti-MRP2 rabbit polyclonal antibody (Zymed Laboratories, San Francisco) in 1:10 dilution overnight at 4 °C. After rinsed 3× with PBS, the samples were incubated with the corresponding secondary antibodies (TRITC-conjugated goat anti-rabbit IgG; FITC-conjugated goat anti-mouse IgG, Invitrogen, Singapore) at RT for 1 h and rinsed 3× with PBS before being mounted in FluorSave[TM] (Calbiochem, CA). The samples were imaged with a Fluoview-300 confocal microscope 15 (Olympus, Japan) using a 63× water-immersion objective (NA1.2).

2.11. Measurement of hepatocyte differentiated functions [32]

All functional data were normalized to 10^6 cells. A Rat Albumin ELISA Quantitation Kit (Bethyl, Texas) was used for the measurement of daily albumin production; urea synthesis of the hepatocyte culture incubated in culture medium with 2 mM NH$_4$Cl for 90 min was measured with Urea Nitrogen Kit (Stanbio, Texas); the 7-ethoxyresorufin-O-deethylation (EROD) assay was initiated by incubating the hepatocytes with 39.2 µM 7-ethoxyresorufin in culture medium at 37 °C for 4 h. The amount of resorufin converted by the enzymes was calculated by measuring the resorufin fluorescence in the incubation medium at 543 nm excitation/570 nm emission against resorufin standards. All the EROD cytochrome P450 1A detoxification activities were normalized relative to freshly isolated hepatocytes.

2.12. Statistical analysis

Results were presented by mean ± standard deviation (M ± S.D.). Each result was statistically analyzed by the t-test. The values of $p < 0.05$ were considered statistically significant.

3. Result

3.1. Fabrication and characterization of bioactive PET TE membranes to construct the synthetic sandwich culture

The synthetic sandwich culture was constructed by a PET-Gal as the bottom substratum and a PET TE membrane (GRGDS-modified or galactosylated or non-modified) as the top support. The entire sandwich construct was secured in the Minusheet Carriers (Fig. 1A).

The fabrication and characterization of the PET-Gal (bottom substratum) were described previously [26]. We fabricated here GRGDS-modified or galactosylated PET TE membranes (top support, Fig. 1B) based on the commercially available PET TE membrane which is naturally hydrophilic with carboxylic and hydroxyl groups presented on the bulk material after the 'track-etching' treatment. The density of the carboxylic groups presented in the non-modified PET TE membrane manufactured by Sterlitech is $5.8 \pm 0.13\,\text{nmol/cm}^2$ as quantified by TBO assay. We further increased the functional carboxylic group density of the membrane to $19.9 \pm 2.5\,\text{nmol/cm}^2$ by oxidization. XPS C 1s core-level peak components of the non-modified PET TE membrane (Fig. 2A) consist of the aromatic carbon (C–H, binding energy (BE) of 284.6 eV), carbon singly bonded to oxygen (C–O, BE of 286.2 eV), and carboxyl carbon (O–C=O, BE of 288.6 eV) in an approximate area ratio of 3.5:1:0.6. The area ratio is slightly different from the chemical structure of PET (with the ratio of 3:1:1) probably due to the particle bombard-ment and alkaline hydrolysis of the polyester bulk material during the 'track etching' treatment. The peak component area associated with the O–C=O species increases in the oxidized PET TE membrane compared with the non-modified PET TE membrane indicating the oxidation of the hydroxyl groups into carboxylic groups, while the area associated with the C–O species decreases accordingly (Fig. 2B).

GRGDS peptide or Gal ligand (AHG) was covalently conjugated onto the oxidized PET TE membrane activated by EDC and sulfo-NHS. C 1s core-level spectra of both the GRGDS-modified and galactosylated PET TE membranes reveal changes in the surface chemical composition after surface modification (Fig. 2A). Successful conjugation of GRGDS peptide or Gal ligand onto the oxidized PET TE membrane was confirmed by the appearance of two new peak components at the BEs of 287.6 and 285.7 eV, attributable to the O=C–NH and the C–N functional groups, respectively, and the substantial decrease in the O–C=O peak component intensity. The successful conjugation of GRGDS peptide or Gal ligand was also confirmed by XPS wide scanning spectrum (Fig. 2B). In contrast to non-modified and oxidized PET TE membranes, a new peak corresponding to N 1s (BE of 400 eV) introduced by bioactive ligands appeared in the spectra of GRGDS-modified and galactosylated PET TE membranes. The final density of the conjugated GRGDS peptide or Gal ligand on the PET TE membrane quantified by RP-HPLC was $0.62 \pm 0.23\,\text{nmol/cm}^2$ or $1.18 \pm 0.34\,\text{nmol/cm}^2$, which showed ~3% or ~6% surface functionality, respectively.
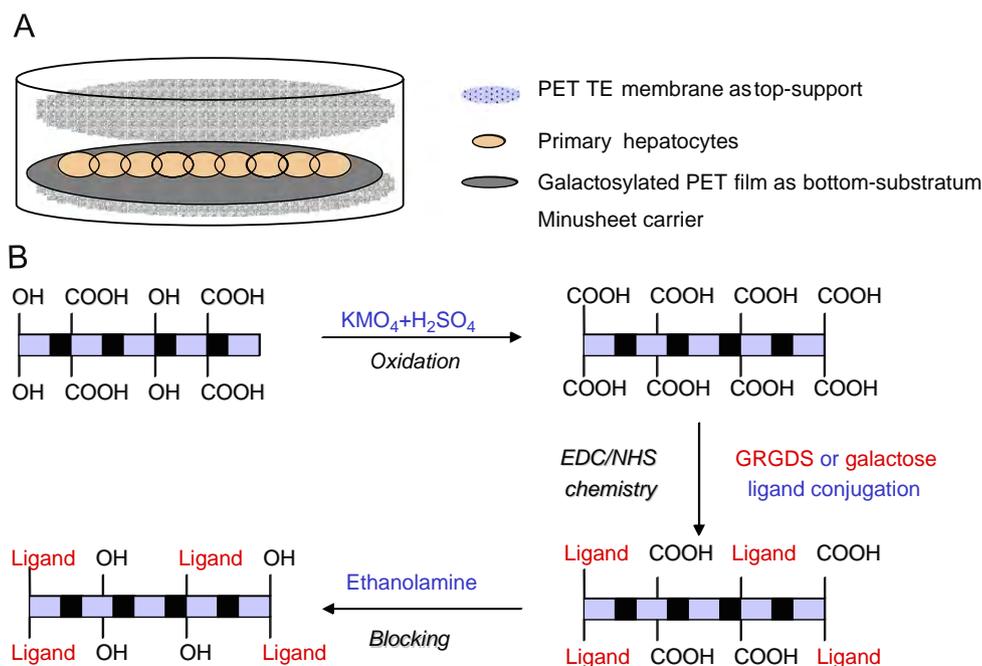
Fig. 1. Schematic diagrams of the synthetic sandwich construct (A) for hepatocyte culture and surface modification method to conjugate GRGDS peptide or galactose ligand onto the PET TE membrane (B).
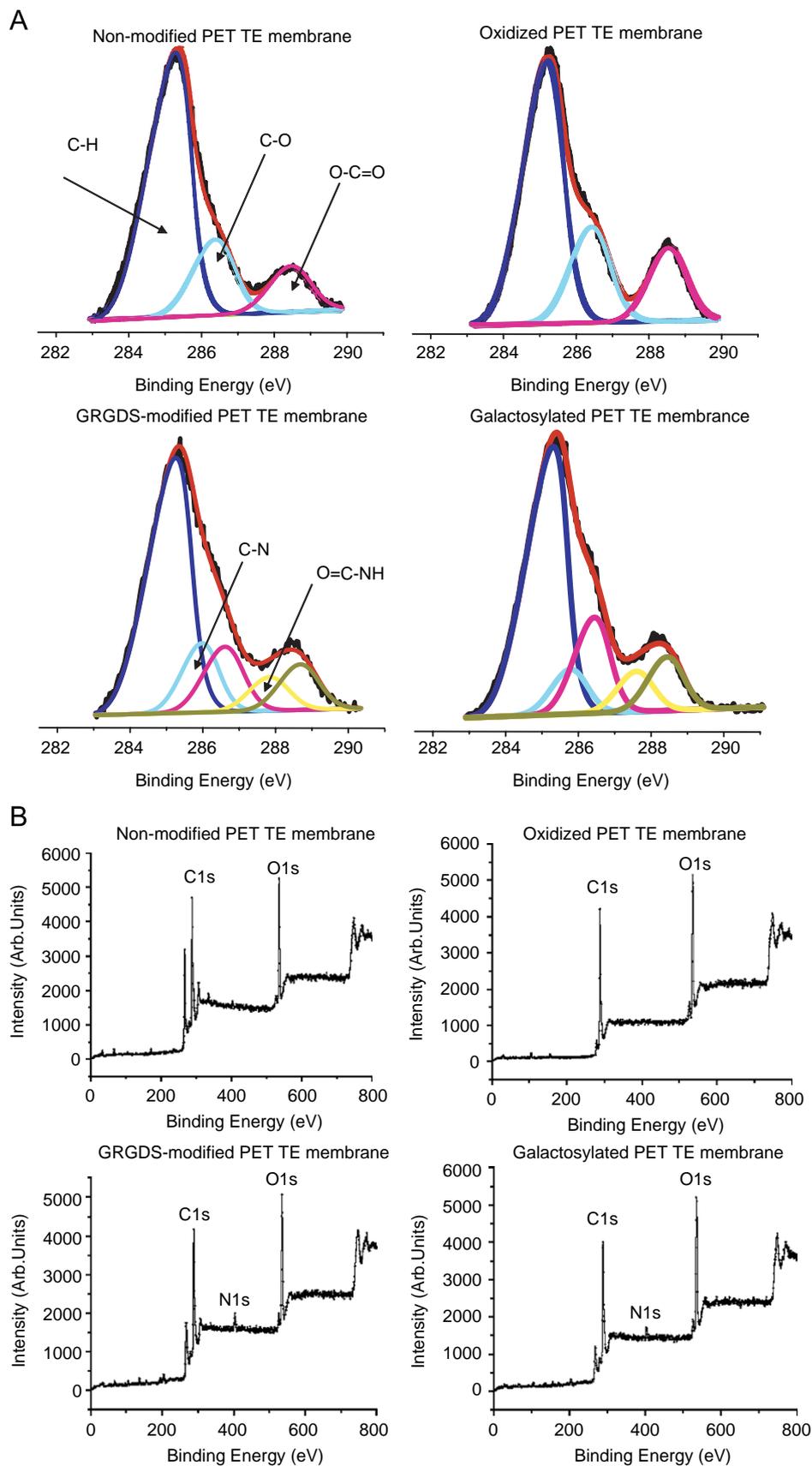
Fig. 2. XPS C 1s core-level spectra (A) and wide scanning spectra (B) of the non-modified PET TE membrane; the oxidized PET TE membrane; GRGDS-modified PET TE membrane and galactosylated PET TE membrane.
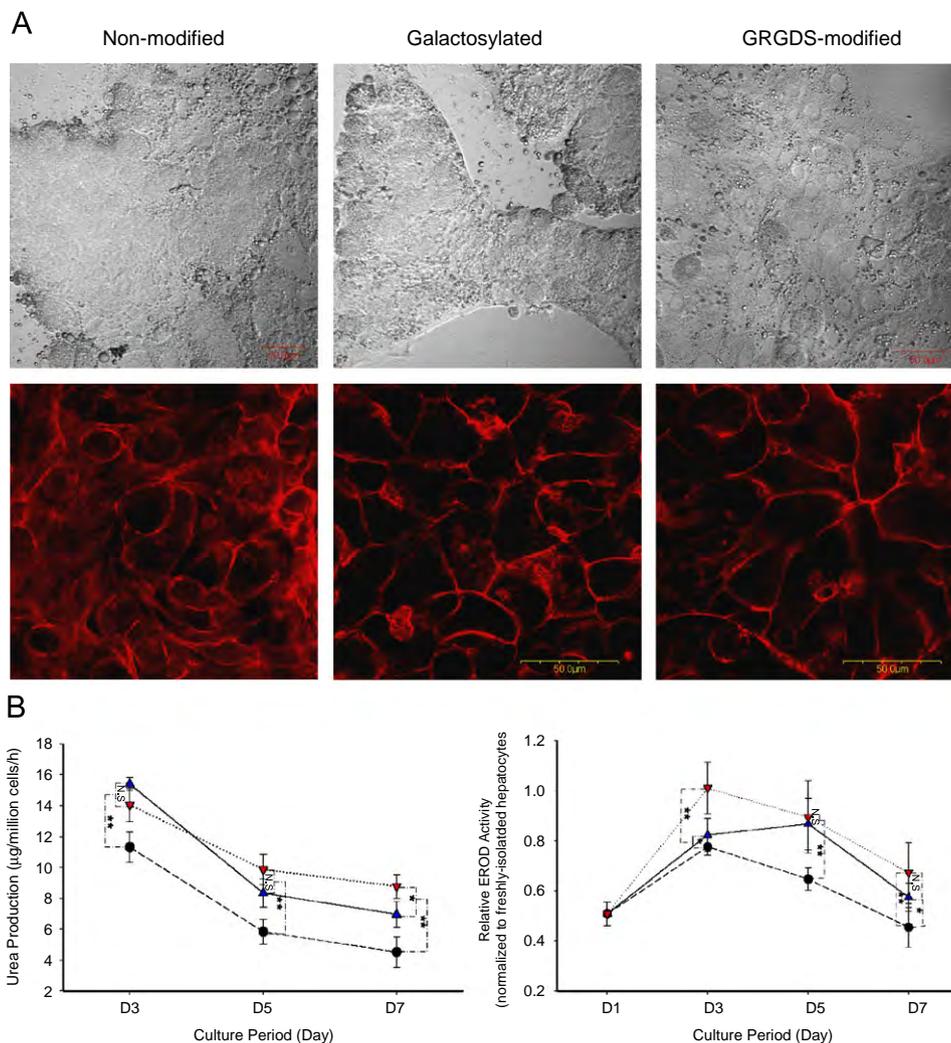
Fig. 3. Effects of the synthetic sandwich culture with three different top supports (galactosylated, GRGDS-modified or non-modified PET TE membrane) on the sandwiched hepatocytes: (A) stabilization of the monolayer morphology (first panel) and F-actin distribution (second panel); (B) hepatocyte differentiated functions in synthetic sandwich culture with ●, non-modified; ▼, GRGDS-modified; ▲, galactosylated PET TE membrane. Data are mean ± S.D., $n = 6$. *, $p < 0.05$; **, $p < 0.01$; NS, not significant.

3.2. Synthetic sandwich culture with various top supports

The synthetic sandwich culture was constructed by overlaying the hepatocytes cultured on the PET-Gal (bottom substratum) with three top supports (galactosylated, GRGDS-modified or non-modified PET TE membrane). As reported previously [19], hepatocytes cultured on the PET-Gal formed a 3D hepatocyte monolayer between day 1 and day 3 after cell seeding (prior to hepatocyte spheroid formation), which exhibited improved cell polarity, cell–cell interactions, and enhanced differentiated functions compared to conventional 2D hepatocyte monolayer on collagen substratum. We investigated here the effects of the 3 top supports on the morphology, cytoskeleton distribution, urea secretion and detoxification functions of the sandwiched 3D hepatocyte monolayer. Top support was overlaid 24 h after seeding hepatocytes onto the PET-Gal when the hepatocytes aggregated into island-like clusters [19]. The sandwiched hepatocytes continuously migrated horizontally; and the island-like clusters merged into a monolayer in the synthetic sandwich culture with all the 3 top supports. Overlaying hepatocytes with galactosylated or GRGDS-modified PET TE membrane induced within 12 h dramatic re-organization of the F-actin from cytosolic distribution into a cortical distribution especially near the cell–cell contact (reminiscent of 3D cell characteristic, [33]); while overlaying with non-modified PET TE membrane did not effectively induce the similar F-actin re-organization (Fig. 3A). After 1-week culture, hepatocyte multi-layers were formed in the synthetic sandwich culture with the galactosylated and non-modified PET TE membrane top supports; while synthetic sandwich culture with the GRGDS-modified PET TE membrane top support could stabilize the hepatocyte monolayer morphology (Fig. 3A). Hepatocytes in the synthetic sandwich culture with the GRGDS-modified PET TE membrane top support exhibited higher urea production and EROD cytochrome P450 1A activity than the

Table 1
Diffusivity of FITC-dextran of various molecular weights across the GRGDS-modified PET TE membrane [PET] and gelled collagen layer [Collagen]

Molecular weights (kDa)	Diffusivity $\times\ 10^8$ (cm^2/s) [PET]	Diffusivity $\times\ 10^8$ (cm^2/s) [Collagen]
9.5	4.58 ± 0.44	2.26 ± 0.56
70	4.38 ± 0.56	2.04 ± 0.69
150	3.53 ± 0.49	1.70 ± 0.53

synthetic sandwich culture with the galactosylated or non-modified PET TE membrane top supports (Fig. 3B). The GRGDS-modified PET TE membrane (top support)/PET-Gal (bottom substratum) synthetic sandwich culture is therefore further characterized for culturing hepatocytes over a period of 2 weeks in comparison with the conventional collagen sandwich culture [7,34].

3.3. Mass transfer in synthetic vs. collagen sandwich cultures

FITC-dextrans with molecular weights of 9.5, 70, and 150 kDa were used to measure the mass transfer across the GRGDS-modified PET TE membrane top support in the synthetic sandwich culture and the gelled-collagen top layer in the collagen sandwich culture. For FITC-dextrans with all the selected sizes, an approximately two-fold increase in mass transfer was observed across the GRGDS-modified PET TE membrane over the gelled-collagen layer (Table 1). The results indicate that the synthetic sandwich culture can achieve better mass transfer between hepatocytes and the culture medium than the collagen sandwich culture.

3.4. Cell morphology and cell–cell interactions in synthetic vs. collagen sandwich cultures

SEM images of hepatocytes maintained in both sandwich cultures 48 h after sandwich assembly were analyzed for cell morphology and cell–cell interactions. 3D hepatocyte monolayer in the synthetic sandwich form tightly organized cell–cell contacts with smooth surface, mimicking the cell–cell interaction pattern in 3D hepatocyte spheroids formed on PET-Gal (Fig. 4A). In contrast, hepatocytes in the collagen sandwich are generally more loosely interacting with each other; and 2D hepatocyte monolayer on the collagen substratum exhibits spreading morphology with clearly demarcated cell-cell boundaries. We further investigated the cell-cell interactions in these four culture conditions by examining the expressions of a cell–cell adhesion protein E-Cadherin (Fig. 4B). The E-Cadherin expression level is the highest in the 3D hepatocyte spheroids on PET-Gal, which is considered as the 'gold-standard' for 3D hepatocyte culture model; followed by the 3D hepatocyte monolayer in the synthetic sandwich culture, which is significantly higher than the E-Cadherin expression level of the hepatocytes in collagen sandwich culture. 3D hepatocyte monolayer in synthetic

sandwich culture therefore enables better cell–cell interactions than the collagen sandwich culture.

3.5. Polarity formation and biliary excretion in synthetic vs. collagen sandwich cultures

A key feature of the sandwich culture is its ability to re-establish *in vivo*-like hepatocyte polarity. In the earlier stage of polarity formation, bile canaliculi are formed between the hepatocytes in concert with changes in cytoskeleton distribution and localization of bile canaliculi transporter MRP2 into the apical domain [35,36]. The cytoskeleton distribution in hepatocytes underwent dramatic changes upon the top support overlaying in both the synthetic and collagen sandwich cultures: F-actin re-organized to the cell–cell contact region from its initial random distribution 12 h after overlaying, which resembles the F-actin distribution *in vivo* [33] (Fig. 5); 24 h after overlaying, extensive and contiguous tight junctions between cells have been established with majority of the MRP2 co-localized to the bile canaliculi formed by contiguous cells, suggesting the preservation of the polarized phenotype (Fig. 5). Our observations indicate comparable hepatic polarity formation of the 3D hepatocyte monolayer in the synthetic sandwich culture as the hepatocytes in the collagen sandwich culture.

The establishment of cell polarity and functional activity of bile canaliculi can be represented by the biliary excretion of hepatocytes, which is an important function of the liver to excrete metabolites and toxins from the body [7]. We examined the dynamic changes of hepatocyte biliary excretion in both sandwich cultures with a non-fluorescent substrate, FDA. FDA enters the cells via passive diffusion; and is hydrolyzed by intracellular esterases into fluorescein before excretion by bile canaliculi transporter (MRP2) [37]. The dynamics of FDA excretion in the 3D hepatocyte monolayer in the synthetic sandwich was similar to the observation from the hepatocytes in the collagen sandwich (Fig. 6). In both sandwich cultures, there was no fluorescein concentrated in bile canaliculi sacs between hepatocytes after 12 h overlaying of the top support; the fluorescein secreted into bile canaliculi sacs began to appear after 24 h overlaying and fully developed between 48 and 72 h (Fig. 6). The fluorescein localized in the intercellular sacs between hepatocytes was quantified by image processing (Fig. 6 and S, see supplementary material). The results indicate that the 3D hepatocyte monolayer in the
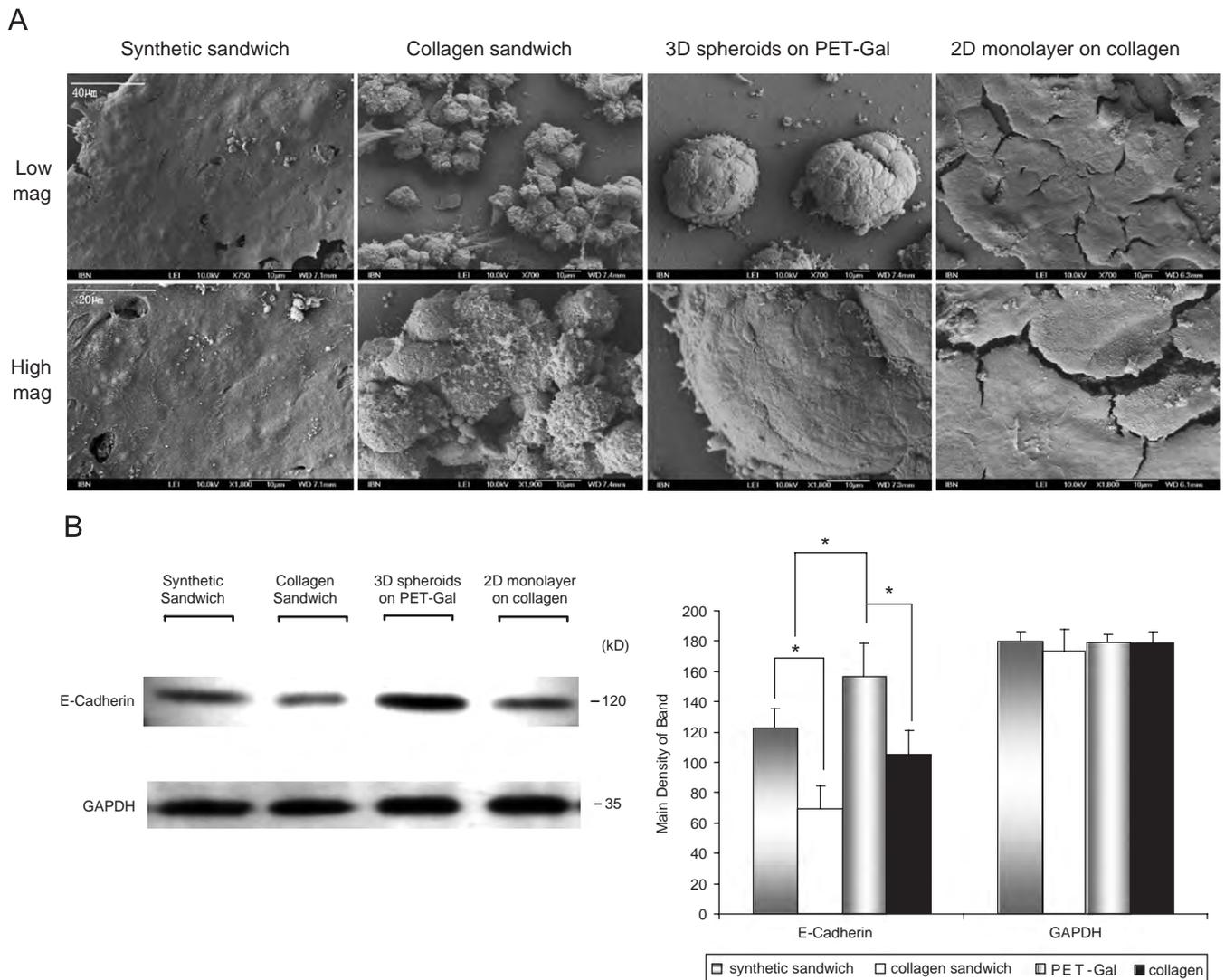
Fig. 4. Cell morphology and cell–cell interaction in synthetic vs. collagen sandwich cultures. (A) SEM images of hepatocytes maintained in synthetic and collagen sandwich culture 48 h after top support overlaying as well as the 3D hepatocyte spheroids on PET-Gal and 2D hepatocyte monolayer on collagen substratum at the same time point (low magnification of $\sim \times 700$ at upper panel with scale bar of 40 μm and high magnification of $\sim \times 1800$ at lower panel with scale bar of 20 μm). (B) Western blot and relative quantification of E-Cadherin and GAPDH expression of the hepatocytes cultured in the synthetic sandwich culture, collagen sandwich culture, as 3D spheroids on PET-Gal and as 2D monolayer on collagen; GAPDH expression was used as loading control. Data are mean ± S.D., $n = 3$. *, $p < 0.05$.

synthetic sandwich exhibit similar extent of biliary excretion compared with the hepatocytes in the collagen sandwich.

3.6. Maintenance of hepatocyte differentiated functions in synthetic vs. collagen sandwich cultures

Key representative differentiated functions of hepatocytes in both sandwich cultures were compared (Fig. 7). Albumin secretion, urea production and 7-ethoxyresorufin-O-deethylation cytochrome P450 1A activity of 3D hepatocyte monolayer in the synthetic sandwich culture were significantly higher than that of the hepatocytes in the collagen sandwich culture over 14 days with the most dramatic enhancement observed within the first 4–6 days. The improvement in the hepatocyte functional mainte-

nance in the synthetic sandwich culture may be due to the better cell–cell interaction of the 3D hepatocyte monolayer and improved mass transfer of nutrients and wastes removal across the synthetic top support.

4. Discussion

A novel synthetic sandwich culture was developed by overlaying a 3D hepatocyte monolayer formed on a PET-Gal with a GRGDS-modified PET TE membrane top support. This 3D hepatocyte monolayer has been characterized previously with improved cellular structure and polarities, enhanced cell–cell interactions, better differentiated functions compared to the hepatocyte monolayer on collagen-coated substratum. Due to the weak adhesive force obtained from the bottom galactosylated substratum
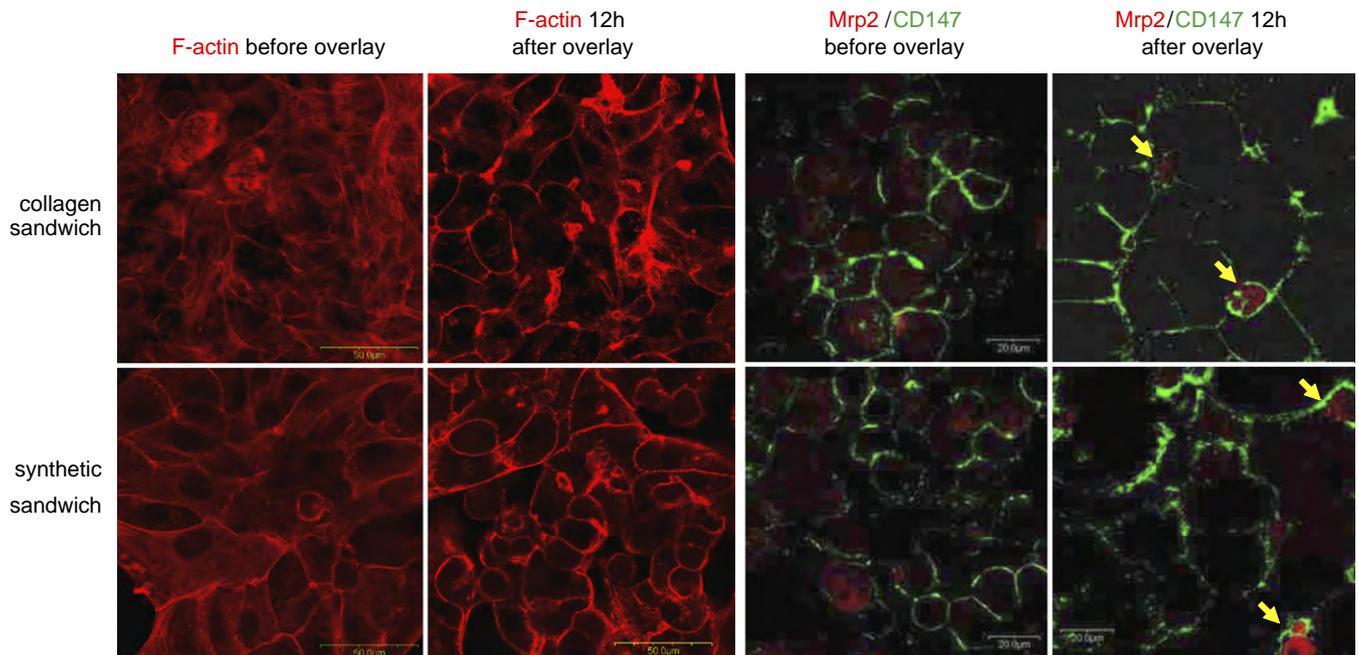
Fig. 5. Polarity formation in synthetic vs. collagen sandwich cultures: representative confocal images of F-actin staining and MRP2/CD147 double-staining of hepatocytes in both sandwich cultures before and after top support overlaying (co-localization of the MRP2 to the bile canaliculi is marked by the arrows).
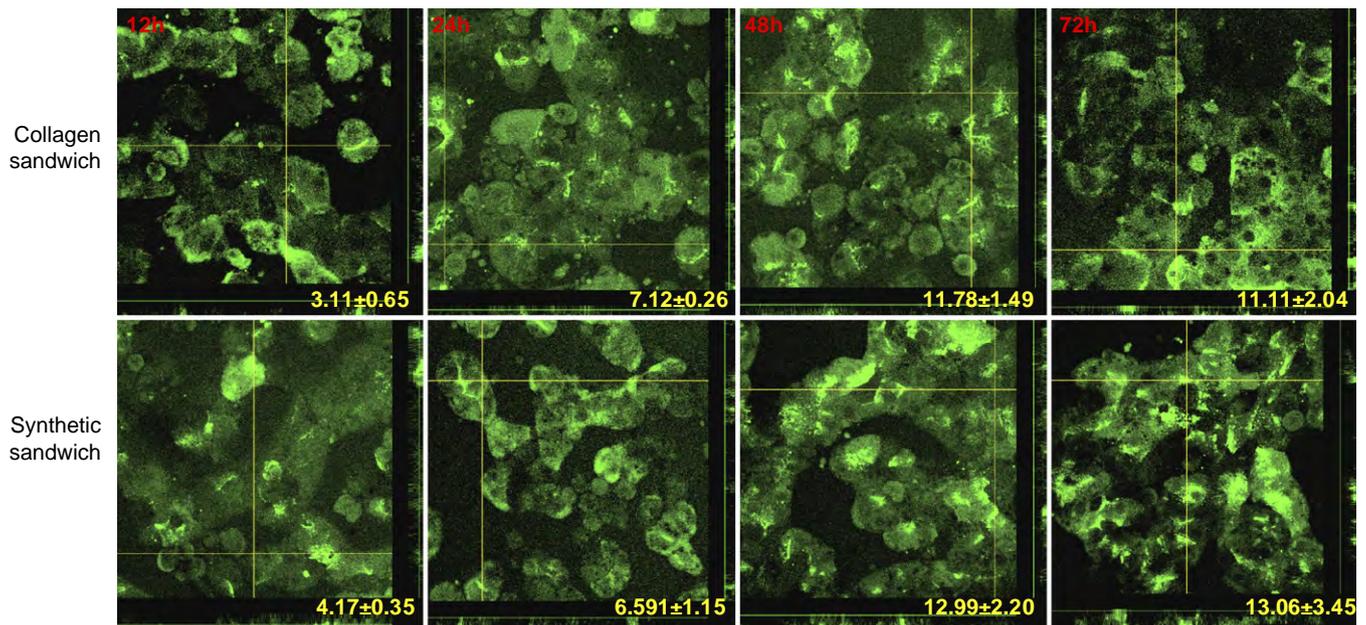
Fig. 6. Biliary excretion of hepatocytes in synthetic vs. collagen sandwich cultures: representative confocal images of dynamic changes of fluorescein excreted by bile canaliculi transporter. The fluorescein localization in the inter-cellular sacs between hepatocytes is quantified as shown by the number at the corner of each image (using an image processing method stated in the supplementary material).

as well as cellular contractions, this 3D hepatocyte monolayer will finally transform to 3D spheroid after 3 days. The GRGDS-modified PET TE membrane top support may act as (1) a mechanical force applied to the hepatocytes from top, which might enhance the cell–substratum interaction and acts as a balance to the cell–cell interaction to stabilize the monolayer morphology [38];

(2) a physical boundary on top of the hepatocyte monolayer to confine the space, which prohibits the monolayer from folding into multi-layer structure in spheroids; (3) a biochemical support with the immobilized bioactive components for morphological and functional improvement. As the non-modified PET TE membrane top support had little effect on stabilizing the hepatocyte

Fig. 7. Hepatocyte functional maintenance in synthetic vs. collagen sandwich cultures as represented by (A) urea production; (B) albumin secretion; (C) normalized EROD cytochrome P450 1A detoxification activity relative to freshly isolated hepatocytes. ●, synthetic sandwich; ▲, collagen sandwich. Data are mean $\pm$ SD, $n = 6$. *, $p < 0.05$; **, $p < 0.01$; NS, not significant.

d–receptor interaction between the galactose and asialoglycoprotein receptor (ASGPR) was relatively weak [39] and hepatocytes cultured in galactosylated substrata tended to form multi-cellular spheroids. RGD–integrin interactions have been shown to induce downstream signaling leading to the redistribution of the cytoskeleton, formation of focal adhesion complex, and enhancement of cell–cell interaction [40,41]. Hepatocytes attached to RGD-modified substrata exhibit a spreading morphology as monolayer, with similar phenotypes as monolayer formed on collagen [42]. When hepatocytes are exposed to GRGDS peptide or galactose ligand on the top support and galactose ligand on the bottom substratum in the synthetic sandwich, the synergistic interplay between these two ligand–receptor interactions is expected. GRGDS-modified PET TE membrane (top support)/PET-Gal (bottom substratum) synthetic sandwich culture performed the best in terms of morphology stabilization, functional maintenance and polarity formation. The GRGDS-modified PET TE membrane top support might induce integrin-mediated cell–matrix interactions on the top support; thus prevent the 3D spheroid formation and stabilize the 3D hepatocyte monolayer morphology. The galactosylated PET TE membrane top support has a poorer stabilization effect on the 3D hepatocyte monolayer, which might be caused by the weaker interaction between the galactose and ASGPR.

We have also investigated the optimal procedure for overlaying the top support onto the 3D hepatocyte monolayer culture. Since the hepatocytes on the bottom PET-Gal film formed island-like clusters on day 1 after seeding and gradually merged into the 3D hepatocyte monolayer on day 2 [19], we overlaid the GRGDS-modified PET TE membrane top support on day 1 and day 2, respectively; and observed no distinct morphological differences over the 2-week culture (data not shown). We therefore overlaid the top support on day 1 to be consistent with the time of overlaying collagen top layer in the collagen sandwich. The hepatocytes within the synthetic sandwich are able to migrate laterally and interact with each other.

The synthetic sandwich exhibits several advantages over the conventional collagen sandwich: (1) minimizing mass transfer barrier caused by the gelled-ECM top layer, which hinders the exchange of nutrients, metabolites, xenobiotics or biochemical signals with the bulk of the medium; (2) mass transfer properties of the synthetic sandwich culture could be readily controlled by choosing commercial PET TE membranes with pore sizes ranging 0.1 μm-10 μm and densities ranging 10^5–10^8 pores/cm^2 (the surface modification of the PET TE membrane with bioactive ligand will not affect the property of bulk material). The improved and controllable mass transfer achieved in the synthetic sandwich culture would be especially important for hepatocyte-based xenobiotics testing [43] and hepatocyte sandwich culture under perfusion condition in the bioreactor [44]. We expect that the improved mass transfer

monolayer and inducing the F-actin re-organization (Fig. 3A), we deduced that the immobilized bioactive ligand (galactose ligand or GRGDS peptide) on the top support play an essential role to achieve morphological and functional maintenance. It is known that the ligan-

in the synthetic sandwich would be maintained during the first few days' culture due to the sparse secretion of ECM by hepatocytes *in vitro* [45]. As indicated in Fig. 4A, few ECMs were observable in either the synthetic sandwich or collagen sandwich after 3-day culture, with most of the ECMs deposited around the cell surface. (3) 3D hepatocyte monolayer in synthetic sandwich exhibited enhanced cell–cell interaction and better differentiated functions maintained for 2 weeks compared to the hepatocytes in collagen sandwich, which may be partially due to the differences between the 3D hepatocyte monolayer on the galactosylated substrata and the 2D hepatocyte monolayer on the collagen substratum before overlaying of the top support. The specific galactose–ASGPR interaction may also play an active role to induce downstream cell-signaling for hepatocyte functional improvement; (4) more homogeneous hepatocyte morphology was observed in the synthetic sandwich culture than in the collagen sandwich culture, which might be due to the uniformity of the bioactive ligands exposed to the cells in the synthetic sandwich culture since it is not easy to produce uniform collagen coating on surfaces. The uniformity of hepatocyte behaviors would be important for mechanism studies using hepatocyte sandwich *in vitro* cultures, such as the studies of hepatic transport and biliary clearance responsible for the accumulation and excretion of a wide variety of drugs [7,8]. We did not observe any significant difference in polarity formation and biliary excretion between the synthetic and collagen sandwich indicating that the nature of the substrata may not be critical for hepatic polarities, as also mentioned by other studies [5,8].

5. Conclusions

We have established an ECM-free synthetic sandwich culture by maintaining a 3D hepatocyte monolayer between a GRGDS-modified PET TE membrane (top support) and a PET-Gal (bottom substratum). The 3D hepatocyte monolayer in the synthetic sandwich culture exhibited similar polarity formation, improved mass transfer, enhanced cell–cell interactions and higher differentiated functions compared with the hepatocytes in the conventional collagen sandwich culture. This synthetic sandwich culture can potentially be used as an alternative to the ECM-based sandwich culture for relevant hepatocyte-based applications in liver tissue engineering and drug discovery.

Acknowledgments

Appendix A. Supplementary material

Supplementary data associated with this article can be found in the online version at doi:10.1016/j.biomaterials.2007.09.016.

References

[1] Dunn JC, Yarmush ML, Koebe HG, Tompkins RG. Hepatocyte function and extracellular matrix geometry: long-term culture in a sandwich configuration. Faseb J 1989;3(2):174–7.

[2] Hughes RC, Stamatoglou SC. Adhesive interactions and the metabolic activity of hepatocytes. J Cell Sci Suppl 1987;8:273–91.

[3] Berthiaume F, Moghe PV, Toner M, Yarmush ML. Effect of extracellular matrix topology on cell structure, function, and physiological responsiveness: hepatocytes cultured in a sandwich configuration. Faseb J 1996;10(13):1471–84.

[4] Bissell DM. Primary hepatocyte culture: substratum requirements and production of matrix components. Fed Proc 1981;40(10):2469–73.

[5] Dunn JC, Tompkins RG, Yarmush ML. Long-term in vitro function of adult hepatocytes in a collagen sandwich configuration. Biotechnol Prog 1991;7(3):237–45.

[6] Dunn JC, Tompkins RG, Yarmush ML. Hepatocytes in collagen sandwich: evidence for transcriptional and translational regulation. J Cell Biol 1992;116(4):1043–53.

[7] Liu X, Chism JP, LeCluyse EL, Brouwer KR, Brouwer KL. Correlation of biliary excretion in sandwich-cultured rat hepatocytes and in vivo in rats. Drug Metab Dispos 1999;27(6):637–44.

[8] Turncliff RZ, Tian X, Brouwer KL. Effect of culture conditions on the expression and function of Bsep, Mrp2, and Mdr1a/b in sandwich-cultured rat hepatocytes. Biochem Pharmacol 2006;71(10):1520–9.

[9] Nussler AK, Wang A, Neuhaus P, Fischer J, Yuan J, Liu L, et al. The suitability of hepatocyte culture models to study various aspects of drug metabolism. Altex 2001;18(2):91–101.

[10] Allen JW, Hassanein T, Bhatia SN. Advances in bioartificial liver devices. Hepatology 2001;34(3):447–55.

[11] LeCluyse EL, Audus KL, Hochman JH. Formation of extensive canalicular networks by rat hepatocytes cultured in collagen-sandwich configuration. Am J Physiol 1994;266(1):1764–74.

[12] Langer R, Tirrell DA. Designing materials for biology and medicine. Nature 2004;428(6982):487–92.

[13] De Bartolo L, Morelli S, Lopez LC, Giorno L, Campana C, Salerno S, et al. Biotransformation and liver-specific functions of human hepatocytes in culture on RGD-immobilized plasma-processed membranes. Biomaterials 2005;26(21):4432–41.

[14] Carlisle ES, Mariappan MR, Nelson KD, Thomes BE, Timmons RB, Constantinescu A, et al. Enhancing hepatocyte adhesion by pulsed plasma deposition and polyethylene glycol coupling. Tissue Eng 2000;6(1):45–52.

[15] Reyes CD, Garcia AJ. Engineering integrin-specific surfaces with a triple-helical collagen-mimetic peptide. J Biomed Mater Res A 2003;65(4):511–23.

[16] Cho CS, Seo SJ, Park IK, Kim SH, Kim TH, Hoshiba T, et al. Galactose-carrying polymers as extracellular matrices for liver tissue engineering. Biomaterials 2006;27(4):576–85.

[17] Kim SH, Goto M, Akaike T. Specific binding of glucose-derivatized polymers to the asialoglycoprotein receptor of mouse primary hepatocytes. J Biol Chem 2001;276(38):35312–9.

[18] Schnaar RL, Weigel PH, Kuhlenschmidt MS, Lee YC, Roseman S. Adhesion of chicken hepatocytes to polyacrylamide gels derivatized with N-acetylglucosamine. J Biol Chem 1978;253(21):7940–51.

[19] Du Y, Han R, Ng S, Ni J, Sun W, Wohland T, et al. Identification and characterization of a novel pre-spheroid 3D hepatocyte monolayer on galactosylated substratum. Tissue Eng 2007;13(7):1455–68.

[20] Moghe PV, Berthiaume F, Ezzell RM, Toner M, Tompkins RG, Yarmush ML. Role of extracellular matrix composition and configuration in maintenance of hepatocyte polarity and function. Biomaterials 1996;17:373–85.

[21] Musat AI, Sattler CA, Sattler GL, Pitot HC. Reestablishment of cell polarity of rat hepatocytes in primary culture. Hepatology 1993; 18(1):198–205.

[22] Mingoia RT, Nabb DL, Yang CH, Han X. Primary culture of rat hepatocytes in 96-well plates: effects of extracellular matrix configuration on cytochrome P450 enzyme activity and inducibility, and its application in in vitro cytotoxicity screening. Toxicol In Vitro 2007;21(1):165–73.

[23] Findeis MA. Stepwise synthesis of a GalNAc-containing cluster glycoside ligand of the asialoglycoprotein receptor. Int J Pept Protein Res 1994;43(5):477–85.

[24] Weigel PHMN, Roseman S, Lee YC. Preparation of 6-aminohexyl D-aldopyranosides. Carbohydr Res 1979;70:83–91.

[25] Ying L, Yin C, Zhuo RX, Leong KW, Mao HQ, Kang ET, et al. Immobilization of galactose ligands on acrylic acid graft-copolymerized poly(ethylene terephthalate) film and its application to hepatocyte culture. Biomacromolecules 2003;4(1):157–65.

[26] Du Y, Chia SM, Han R, Chang S, Tang H, Yu H. 3D hepatocyte monolayer on hybrid RGD/galactose substratum. Biomaterials 2006;27(33):5669–80.

[27] Pan X, Aw C, Du Y, Yu H, Wohland T. Characterization of poly(acrylic acid) diffusion dynamics on the grafted surface of poly(ethylene terephthalate) films by fluorescence correlation spectroscopy. Biophys Rev Lett 2006;1(4):433.

[28] Marchand-Brynaert J, Detrait E, Noiset O, Boxus T, Schneider YJ, Remacle C. Biological evaluation of RGD peptidomimetics, designed for the covalent derivatization of cell culture substrata, as potential promotors of cellular adhesion. Biomaterials 1999;20(19):1773–82.

[29] Uchida EYU, Ikada Y. Sorption of low-molecular-weight anions into thin polycation layers grafted onto a film. Langmuir 1993;9:1121–4.

[30] Seglen PO. Preparation of isolated rat liver cells. Methods Cell Biol 1976;13:29–83.

[31] Dong LC, Hoffman AS, Yan Q. Dextran permeation through poly(N-isopropylacrylamide) hydrogels. J Biomater Sci Polym Ed 1994;5(5):473–84.

[32] Ng S, Han R, Chang S, Ni J, Hunziker W, Goryachev AB, et al. Improved hepatocyte excretory function by immediate presentation of polarity cues. Tissue Eng 2006;12(8):2181–91.

[33] Hamilton GA, Jolley SL, Gilbert D, Coon DJ, Barros S, LeCluyse EL. Regulation of cell morphology and cytochrome P450 expression in human hepatocytes by extracellular matrix and cell–cell interactions. Cell Tissue Res 2001;306(1):85–99.

[34] LeCluyse EL, Audus KL, Hochman JH. Formation of extensive canalicular networks by rat hepatocytes cultured in collagen–sandwich configuration. Am J Physiol 1994;266(6, Pt 1):C1764–74.

[35] Yeaman C, Grindstaff KK, Nelson WJ. New perspectives on mechanisms involved in generating epithelial cell polarity. Physiol Rev 1999;79(1):73–98.

[36] Hoffmaster KA, Turncliff RZ, LeCluyse EL, Kim RB, Meier PJ, Brouwer KL. P-glycoprotein expression, localization, and function in sandwich-cultured primary rat and human hepatocytes: relevance to the hepatobiliary disposition of a model opioid peptide. Pharm Res 2004;21(7):1294–302.

[37] LeBlanc GA. Hepatic vectorial transport of xenobiotics. Chem Biol Interact 1994;90(2):101–20.

[38] Powers MJ, Griffith LG. Adhesion-guided in vitro morphogenesis in pure and mixed cell cultures. Microsc Res Tech 1998;43(5): 379–84.

[39] Lodish HF. Recognition of complex oligosaccharides by the multi-subunit asialoglycoprotein receptor. Trends Biochem Sci 1991;16(10): 374–7.

[40] Pinkse GG, Jiawan-Lalai R, Bruijn JA, de Heer E. RGD peptides confer survival to hepatocytes via the beta1-integrin-ILK-pAkt pathway. J Hepatol 2005;42(1):87–93.

[41] Fittkau MH, Zilla P, Bezuidenhout D, Lutolf MP, Human P, Hubbell JA, et al. The selective modulation of endothelial cell mobility on RGD peptide containing surfaces by YIGSR peptides. Biomaterials 2005;26(2):167–74.

[42] Bhadriraju K, Hansen LK. Hepatocyte adhesion, growth and differentiated function on RGD-containing proteins. Biomaterials 2000;21(3):267–72.

[43] Walker TM, Rhodes PC, Westmoreland C. The differential cytotoxicity of methotrexate in rat hepatocyte monolayer and spheroid cultures. Toxicol In Vitro 2000;14(5):475–85.

[44] De Bartolo L, Jarosch-Von Schweder G, Haverich A, Bader A. A novel full-scale flat membrane bioreactor utilizing porcine hepatocytes: cell viability and tissue-specific functions. Biotechnol Prog 2000;16(1):102–8.

[45] Arnaud A, Fontana L, Angulo AJ, Gil A, Lopez-Pedrosa JM. Proliferation, functionality, and extracellular matrix production of hepatocytes and a liver stellate cell line: a comparison between single cultures and cocultures. Dig Dis Sci 2003;48(7):1406–13.